

Long-term trends and drivers of aerosol pH in eastern China

Min Zhou^{1,2}, Guangjie Zheng³, Hongli Wang¹, Liping Qiao¹, Shuhui Zhu¹, Dandan Huang¹, Jingyu An¹,
Shengrong Lou¹, Shikang Tao¹, Qian Wang¹, Rusha Yan¹, Yingge Ma¹, Changhong Chen¹, Yafang Cheng³,
Hang Su^{*,1,4}, Cheng Huang¹

¹State Environmental Protection Key Laboratory of the Cause and Prevention of Urban Air Pollution
Complex, Shanghai Academy of Environmental Sciences, Shanghai 200233, China

²School of Atmospheric Sciences, Nanjing University, Nanjing 210023, China

³Minerva Research Group, Max Planck Institute for Chemistry, Mainz 55128, Germany

⁴Multiphase Chemistry Department, Max Planck Institute for Chemistry, Mainz 55128, Germany

*Corresponding author: Hang Su (h.su@mpic.de)

Abstract

Aerosol acidity plays a key role in regulating the chemistry and toxicity of atmospheric aerosol particles. The trend of aerosol pH and its drivers are crucial in understanding the multiphase formation pathways of aerosols. Here, we reported the first trend analysis of aerosol pH from 2011 to 2019 in eastern China. The implementation of the Air Pollution Prevention and Control Action Plan leads to -35.8%, -37.6%, -9.6%, -81.0% and 1.2% changes of $\text{PM}_{2.5}$, SO_4^{2-} , NH_x , non-volatile cations (NVCs) and NO_3^- in Yangtze River Delta (YRD) region during this period. Different from the fast changes of aerosol compositions due to the implementation of the Air Pollution Prevention and Control Action Plan, aerosol pH ~~shows~~ showed a moderate change of -0.24 unit over the 9 years. Besides the multiphase buffer effect, the opposite effects from the changes of SO_4^{2-} and non-volatile cations ~~changes~~ played key roles in determining the moderate pH trend, contributing to a change of +0.38 and -0.35 unit, respectively. Seasonal variations in aerosol pH were mainly driven by the temperature, while the diurnal variations were driven by both temperature and relative humidity. In the future, SO_2 , NO_x and NH_3 emissions are expected to be further reduced by 86.9%, 74.9% and 41.7% in 2050 according to the best health effect pollution control scenario (SSP1-26-BHE). The corresponding aerosol pH in eastern China is estimated to increase by ~0.9, and the reduction in particle phase NO_3^- and NH_4^+ is less than the reduced amount of total HNO_3 and total NH_3 , resulting in 8% more NO_3^- and 35% less NH_4^+ partitioning/formation in the aerosol phase, which This suggests a largely-reduced benefit of NH_3 and NO_x emission control in mitigating haze pollution in eastern China.

设置了格式: 字体: 10 磅

1 Introduction

Aerosol acidity is an important parameter in atmospheric chemistry studies. It affects the particle mass and chemical composition by regulating the reactions of aerosols, and is closely associated with human health, ecosystems and climate (Li et al., 2017; Nenes et al., 2020b; Pye et al., 2020; Su et al., 2020). Aerosol acidity has attracted an increasing concern in recent years because of its impacts on the thermodynamics of gas-particle partitioning, pH-dependent condensed-phase reactions and trace metal solubility (Cheng et al., 2016; Fang et al., 2017; Guo et al., 2017b; Guo et al., 2016; He et al., 2018; Song

et al., 2018; Weber et al., 2016; Su et al., 2020; [Tilgner et al., 2021](#)).

Aerosol pH is normally estimated using thermodynamic models, such as E-AIM(Clegg et al., 1998) and ISORROPIA II, due to the limitations of direct aerosol pH measurement techniques(Fountoukis and Nenes, 2007; Hennigan et al., 2015). The global distribution of aerosol pH generally ranges from 1 to 6(Pye et al., 2020; Zheng et al., 2020; Su et al., 2020). ~~In the United States, A~~aerosols ~~in the United States~~ are ~~reported~~ highly acidic, with pH values of approximately 1–2(Guo et al., 2015; Nah et al., 2018; Pye et al., 2018; Zheng et al., 2020). ~~While A~~aerosols in mainland China and Europe ~~have are less acidic with~~ similar average ~~aerosol acidity~~ levels (~~with pH = ranging between 2.5– and 6~~)(Guo et al., 2018; Jia et al., 2018; Masiol et al., 2020; Shi et al., 2019; Tan et al., 2018; Wang et al., 2019; Zheng et al., 2020).

Aerosol pH exhibits notable spatial and temporal variability, which is affected by changes in factors such as temperature, relative humidity (RH), and aerosol compositions(Pye et al., 2018; Nenes et al., 2020a; Tao et al., 2020; Zheng et al., 2020). Very few studies have investigated the trend and spatial variability of aerosol pH and its drivers. Weber et al.(Weber et al., 2016) showed that aerosols ~~tended~~ to remain highly acidic upon the reduction of SO_4^{2-} during summertime in the southeastern United States. Based on the 10-year observations in six Canadian sites, Tao and Murphy (Tao and Murphy, 2019) suggested that meteorological parameters ~~are were~~ more important than the chemical compositions in controlling aerosol pH variations. Zheng et al.(Zheng et al., 2020) found that aerosol liquid water content (ALWC) and temperature ~~are were~~ the main factors that contribute to the pH difference between the wintertime North China Plain and summertime southeastern United States, whereas the change of chemical composition only ~~plays played~~ a minor role (15%). In China, the trend of aerosol pH and its drivers remain poorly understood, especially in recent years when the emissions and aerosol compositions undergo substantial changes.

To tackle severe particulate matter pollution in China, the Chinese government released the Air Pollution Prevention and Control Action Plan (hereinafter referred to as the Action Plan) in September 2013, which is the first plan to specify air quality goals in China(Cai et al., 2017; Liu et al., 2018; Zheng et al., 2018). The implementation of the Action Plan has led to significant changes in the concentrations and chemical characteristics of fine particulate ($\text{PM}_{2.5}$). Aerosol pH may change due to the significant changes of the chemical composition in $\text{PM}_{2.5}$, which may feedback to the multiphase formation pathways of aerosols such as sulfate, nitrate and ammonium.(Cheng et al., 2016; [Vasilakos et al., 2018](#);

Nenes et al., 2020a).

In this study, we performed a comprehensive analysis of the long-term trends of aerosol pH and its drivers in the Yangtze River Delta of eastern China. ~~In this study, a~~ thermodynamic model, ISORROPIA II (version 2.1) (Fountoukis and Nenes, 2007) was applied to estimate the pH based on 9-year continuous online measurements of PM_{2.5} compositions at an urban site in Shanghai. The main purposes of this study ~~were~~ are to: (1) ~~characterizing~~ characterize the long-term trend ~~in~~ of aerosol pH; (2) investigate the seasonal and diurnal variations of aerosol pH and the main factors that affect these changes and (3) predict further pH under different emission control scenarios and its impact on the formation of ammonium and nitrate. The results presented here may help to advance our understanding ~~of~~ in aerosol chemistry in China and support the development of effective pollution control strategy.

2 Material and Methods

2.1 Ambient measurements

The observational site in this study is located ~~in~~ at the Shanghai Academy of Environmental Sciences (SAES, 31°10'N, 121°25'E), a mixed commercial and residential district in the southwest central urban area of Shanghai (Fig. S1). In the absence of a significant nearby industrial source, this sampling site can be regarded as a representative urban area influenced by a wide mixture of emission sources. A detailed description can be found in previous studies (Qiao et al., 2014; Zhou et al., 2016).

The sampling was conducted from 2011 to 2019. Hourly mass concentrations of water-soluble gases (HCl, HNO₂, SO₂, HNO₃, NH₃) and major water-soluble inorganic ions in PM_{2.5}, including SO₄²⁻, nitrate (NO₃⁻), chloride (Cl⁻), ammonium (NH₄⁺), sodium (Na⁺), potassium (K⁺), calcium (Ca²⁺) and magnesium (Mg²⁺), were measured using an on-line analyser to monitor aerosols and gases (MARGA ADI 2080, Applikon Analytical B.V). ~~The~~ dDetails of measurements were given in Qiao et al. (Qiao et al., 2014). To better track the retention time changes of different ion species and ensure their concentrations ~~to be~~ were measured successfully, an internal ~~standard check~~ calibration was conducted every hour with Lithium Bromide (LiBr) standard solution (Qiao et al., 2014; Zhou et al., 2016). In addition, cleaning the sampling system of MARGA and the multi-points calibrations with the standard solutions were performed every three months to ensure the accuracy of MARGA. Figure S2 compares the sum of SO₄²⁻, NO₃⁻ and Cl⁻ with the sum of NH₄⁺, Na⁺, K⁺, Ca²⁺ and Mg²⁺ in neq/m³ to check the

charge balance. Data in 2011-2016 were more scattered than that in 2017-2019, mainly due to the significant decreases in Ca^{2+} , K^+ and Mg^{2+} from 2011 to 2019 (Fig S3-S5). The correlation between cation and anion was strong ($R^2=0.94$), with a slope of 1.00, indicating that these ion species represented were charge balanced and well represented the major ions components in $\text{PM}_{2.5}$, and the anion and cation were charge balanced. In previous studies, intercomparison experiments between MARGA and filter-based method have been carried out, and the data measured by MARGA showed acceptable accuracy and precision (Rumsey et al., 2014; Huang et al., 2014; Stieger et al., 2018). The mass concentrations of $\text{PM}_{2.5}$ were simultaneously measured using an on-line beta attenuation PM monitor (FH 62 C14 series, Thermo Fisher Scientific) using beta attenuation techniques at a time resolution of 5 min. The temperature and RH were also measured using meteorological parameters monitor (Metone 579, Met One Instruments) at a time resolution of 1 min.

2.2 Aerosol pH prediction

The aerosol pH was predicted using the ISORROPIA II thermodynamic model (Fountoukis and Nenes, 2007). ISORROPIA II can calculate the equilibrium H_{air}^+ and aerosol liquid water content of inorganic material ($ALWC_i$) by inputting the concentrations of the total SO_4^{2-} (TH_2SO_4 , replaced by observed SO_4^{2-}), total NO_3^- (TNO_3 , gas HNO_3 plus particle NO_3^-), total ammonia (NH_x , gas NH_3 plus particle NH_4^+), total Cl^- (TCl , replaced by observed Cl^- due to the low concentration and measurement uncertainties of HCl) (Rumsey et al., 2014), non-volatile cations (NVCs, observed Na^+ , K^+ , Ca^{2+} , Mg^{2+}) and meteorological parameters, including (-temperature and RH) (Guo et al., 2016). H_{air}^+ and $ALWC_i$ are then used to obtain the $\text{PM}_{2.5}$ pH by Eq. (1).

$$pH = -\log_{10} H_{aq}^+ \cong -\log_{10} \frac{1000 H_{air}^+}{ALWC_i + ALWC_o} \cong -\log_{10} \frac{1000 H_{air}^+}{ALWC_i}, \quad (1)$$

where H_{aq}^+ is the H^+ concentration in solution (mol/L), H_{air}^+ is the H^+ loading for an air sample ($\mu\text{g}/\text{m}^3$) and $ALWC_i$ and $ALWC_o$ are the aerosol liquid water contents of inorganic and organic species, respectively ($\mu\text{g}/\text{m}^3$). $ALWC_o$ was calculated by Eq. (2) (Guo et al., 2015).

$$ALWC_o = \frac{m_{org} \rho_w}{\rho_{org}} \frac{k_{org}}{\left(\frac{1}{RH} - 1\right)}, \quad (2)$$

where m_{org} is the mass concentration of organic aerosol, ρ_w is the density of water ($\rho_w=1.0\text{g}/\text{cm}^3$),

ρ_{org} is the density of organics ($\rho_{org}=1.4\text{g/cm}^3$)(Guo et al., 2015), and k_{org} is the hygroscopicity parameter of organic aerosol ($k_{org} = 0.087$)(Li et al., 2016). The annual $ALWC_o$ calculated for 2011-2019 in Shanghai were $1.4\text{--}2.5\mu\text{g/m}^3$, only accounting for 4.3%–7.5% of the total aerosol liquid water content. The pH predictions in previous studies were insensitive to $ALWC_o$ unless the mass fraction of $ALWC_o$ to the total aerosol liquid water content was close to unity(Guo et al., 2015). The use of $ALWC_i$ to predict pH is therefore fairly accurate and common(Battaglia et al., 2017; Ding et al., 2019; Battaglia Jr et al., 2019). In this study, ISORROPIA II was run in the forward mode and ‘metastable’ state. Calculations using total (gas and aerosol) measurements in the forward mode are less affected by measurement errors(Hennigan et al., 2015; Song et al., 2018). A detailed description of the pH calculations can be found in previous studies(Guo et al., 2017a; Guo et al., 2015; Song et al., 2018).

Figure S3-S6 compares the predicted and measured concentrations of NH_3 , NH_4^+ , NO_3^- and HNO_3 . The results show that the modelled and measured NH_3 , NH_4^+ and NO_3^- concentrations are in good agreement, with R^2 values above 0.89 and slopes near 1.00, indicating that the thermodynamic analysis accurately represents the aerosol state and that deviations in the calculated pH values are lower than that in modelled NH_3 (Weber et al., 2016). However, the predicted and measured concentrations of HNO_3 show a poor correlation, as reported in previous studies(Ding et al., 2019; Guo et al., 2015). This may be attributed to lower gas-phase concentrations than particle-phase concentrations and the measurement uncertainties of HNO_3 from MARGA(Rumsey et al., 2014). The development of an alternative approach is therefore required to accurately represent HNO_3 .

2.3 Sensitivity analysis and Drivers of aerosol pH variations

To investigate the factors that drive changes in aerosol pH, sensitivity tests of pH to different factors, including temperature, RH, SO_4^{2-} , TNO_3 , NH_3 , Cl^- and NVCs, were performed. Figure S4 shows how these factors affected the aerosol pH. In the sensitivity tests, we found that an elevated temperature and SO_4^{2-} could decrease pH. As shown in Figure S4, particles tend to become more acidic at higher temperatures. The temperature dependence of pH is mainly determined by the phase partitioning of $\text{NH}_3/\text{NH}_4^+$ based on the equilibria $\text{NH}_3(\text{g}) \leftrightarrow \text{NH}_3(\text{aq})$ and $\text{NH}_3(\text{aq}) + \text{H}_2\text{O} \leftrightarrow \text{NH}_4^+ + \text{OH}^-$, which are governed by the temperature-dependent constants K_H and K_b , respectively(Hennigan et al., 2015; Zheng et al., 2020). Figures S4 also show that elevations in NH_3 , NVCs and RH can increase the aerosol pH

设置了格式: 非上标/ 下标

and ALWC. For TNO_3 and Cl^- , we find their impacts on the aerosol pH were rather weak through sensitivity test and thus are not discussed in detail here.

In this study, we also try to quantify the effects of different factors on the annual, seasonal and diurnal variations of aerosol pH to identify the most important determinants. To quantify the effects of individual factors on the aerosol pH, we first estimated the pH by using the ISORROPIA model with initial values of the different factors, including annual, seasonal and hourly mean value of temperature, RH, SO_4^{2-} , TNO_3 , NH_3 , Cl^- and NVCs. We then estimated the changed pH ($\text{pH}_{\text{change}}$) by varying one factor while holding the other factors fixed. The difference in aerosol pH (ΔpH , $\Delta\text{pH} = \text{pH}_{\text{change}} - \text{pH}$) represents the effect of an individual factor change on the aerosol pH.

To investigate the factors that drive changes in aerosol pH, sensitivity tests of pH variations to different factors, including temperature, RH, SO_4^{2-} , TNO_3 , NH_3 , Cl^- and NVCs, were performed with the one-at-a-time method. For illustration, assume the aerosol pH estimated under scenario I (pH_I) differs with that under scenario II (pH_{II}), and the pH difference, $\Delta\text{pH} = \text{pH}_{II} - \text{pH}_I$, are caused by the variations in the factors listed above. To quantify the contributions of individual factors, we varied the factor i from the level in scenario I to that in scenario II while keeping the other factors fixed. The corresponding pH changes, ΔpH_i , are assumed to represent the contribution of this individual factor change to the overall aerosol pH variations. The unresolved contributors to pH differences, i.e., $\Delta\text{pH} - \sum_i \Delta\text{pH}_{i,s}$, are attributed to “others”, which may represent the contribution of covariations between the factors. This method is applied in Fig. 1b, Fig. 3 and Fig. 5, where the corresponding scenarios represent the average conditions in different years (Fig. 1b), seasons (Fig. 3) or diurnal periods (Fig. 5).

3 Results and Discussion

3.1 Long-term trends of aerosol pH

3.1.1 Trends of aerosol pH.

The 9-year time series of aerosol pH calculated by ISORROPIA II is shown in Figure 1a. A declining trend in $\text{PM}_{2.5}$ pH from 3.30 ± 0.58 in 2011 to 3.06 ± 0.55 in 2019 was observed, with the fitted decrease rate of around 0.04 unit pH per year, which may be related to chemical composition changes (Figs. S5S7-S6S8) due to the pollution control measures taken in the Yangtze River Delta (YRD) region. The Chinese

government started to implement the Action Plan, a series of air pollution control policies, in September 2013, which resulted in a ~~clear-obvious~~ decline in $PM_{2.5}$ and its chemical components (Cheng et al., 2019; Li et al., 2019). Compared to the concentrations before the implement of the Action Plan (i.e., 2011-2012 averages), $PM_{2.5}$, SO_4^{2-} , NH_x and NVCs after the implement of the Action Plan (i.e., 2018-2019 averages) decreased by 35.8%, 37.6%, 9.6% and 81.0%, respectively, while NO_3^- increased by 1.2% (Fig. S5S7). In terms of the chemical profiles, SO_4^{2-} , NH_4^+ and NO_3^- remained the most abundant inorganic water-soluble ions, accounting for 83.4%–94.1% of the total ions in $PM_{2.5}$ ~~over the nine years~~. While the proportions of NH_4^+ and NO_3^- increased continuously (increased by 2.2% and 13.1% from 2011 to 2019, respectively), those of NVCs and SO_4^{2-} decreased by 6.0% and 4.6%, respectively. Despite of the substantial change of aerosol abundance and composition, the aerosol pH ~~shows-showed~~ a moderate change. The effects of chemical composition changes in $PM_{2.5}$ on the aerosol pH are further discussed in Section 3.1.2.

The $PM_{2.5}$ in Shanghai was moderately acidic with daily pH ranged from 1.15 to 5.62, similar to those from other cities in China (Shi et al., 2019; Tan et al., 2018). Table S1 shows the ~~aerosol pH data-in other cities or countries obtained~~ from the literatures, which were ~~also~~ calculated using thermodynamic models ~~of different cities in summer and winter~~. In general, ~~the~~ $PM_{2.5}$ pH ~~ranges-level~~ in Chinese cities were higher than those in US cities yet similar to those in European cities.

3.1.2 Driving factors.

Figure 1b shows the contributions of individual factors to the ΔpH from 2011 to 2019. ~~Here the bar plots indicate the factors contributing to the ΔpH between two adjacent scenarios, e.g., 2011 to 2013. See Fig. S9a for the factor contribution to the variation from average conditions.~~ Note that in Fig. 1b, the aerosol pH was calculated from the annual averages of input parameters. This is different from Sect 3.1.1, where the annual pH is the average of hourly values based on hourly observation data. The aerosol pH decreased from 3.35 in 2011 to 3.28 in 2013. The main factors that affected the pH in this period (prior to the implementation of the Action Plan) were the temperature and NVCs. Upon implementation of the Action Plan (2013-2019), the concentrations of $PM_{2.5}$ and its chemical components decreased substantially (Fig. S5S7). ~~Hence~~, the role of the chemical composition in the aerosol pH ~~become~~ ~~became~~ more prominent than the period of 2011-2013. The pH value continuously decreased from 3.28 in 2013 to 3.19 in 2019. Changes ~~in-of~~ SO_4^{2-} and NVCs were more important determinants ~~of-in~~ the

change of aerosol pH, resulting in ΔpH of +0.38 units and -0.35 units from 2013 to 2019, respectively. Besides the effect of reduction in SO_4^{2-} (Fu et al., 2015; Xie et al., 2020), our results suggest that the change in NVCs may also play an important role in determining the trend of aerosol pH. The effects of SO_4^{2-} and NVCs on pH were much weaker during 2017–2019 than during 2013–2017, consistent with the fact that the decline in pollutant concentrations has slowed in recent years (Fig. S6S8). Thus, temperature and NH_x ~~become~~became the main drivers of the ΔpH during 2017–2019.

From 2013 to 2019, changes in the NH_x and Cl^- were associated with 0.08 and 0.06 decreases in ΔpH , respectively, whereas TNO_3 had little effect on the ΔpH . Overall, the changes in SO_4^{2-} and NVCs were the main drivers of the ΔpH under the implemented Action Plan, and NH_x appeared to play an increasingly important role in determining the aerosol pH through the years.

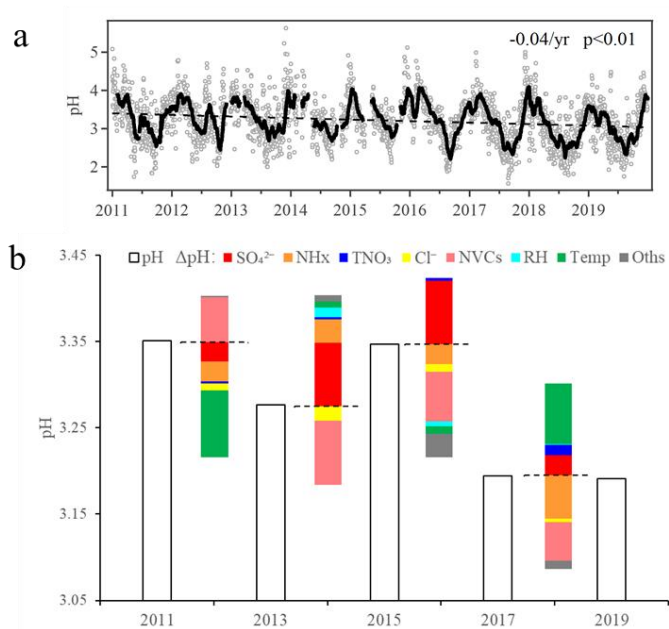


Figure 1. (a) Long-term trends in aerosol pH during 2011–2019 in Shanghai. Gray dots and black lines represent the daily pH values and 30-day moving average pH values, respectively. **(b) Fractional contributions of individual drivers-factors to the ΔpH change in aerosol pH during from 2011–to 2019.** Here the bar plots indicate the factors contributing to the ΔpH between two adjacent scenarios, e.g., 2011 to 2013. The meanings of

带格式的：居中

设置了格式：字体：非加粗

the abbreviations are: RH, relative humidity; Temp, temperature; NVCs, non-volatile cations; NH_x , total ammonia; TNO_3 , total nitrate.

2.2 3.2 Seasonal variation

Figure 2 shows the seasonal variations of aerosol pH in Shanghai. The average pH values were 3.33 ± 0.49 , 2.89 ± 0.49 , 2.99 ± 0.52 and 3.59 ± 0.57 in spring (March–May, MAM), summer (June–August, JJA), fall (September–November, SON) and winter (December–February, DJF), respectively. The highest aerosol pH was found in winter while the lowest pH was found in summer. This is with similar seasonal trend but generally lower levels than that observed in Beijing and other NCP cities (Tan et al., 2018; Ding et al., 2019; Shi et al., 2019; Wang et al., 2020), due to the generally lower aerosol concentrations in YRD.

Figure 3 shows the contributions of individual factors to the ΔpH across the four seasons. Here the bar plots indicate the factors contributing to the ΔpH between two adjacent seasons, e.g., spring (MAM) to summer (JJA). See Fig. S9b for the factor contribution to the variation from average conditions. The aerosol pH was calculated from the mean averages of input parameters in four seasons, and the ΔpH was estimated by varying one factor while holding the other factors fixed in different seasons. According to the multiphase buffer theory, the peak buffer pH, $\text{p}K_a^*$ regulates the aerosol pH in a multiphase-buffered system, and temperature can largely drive the seasonal variation of aerosol pH through its impact on $\text{p}K_a^*$ (Zheng et al., 2020). Figure 3 confirms this conclusion, and shows a dominant role of temperature in driving the seasonal variation of aerosol pH. The temperature was associated with a max ΔpH of 0.63 from fall to winter. Besides temperature, the main factors affecting aerosol pH are NH_x and SO_4^{2-} (Fig. 3), contributing 16% and 12% of the changes, respectively. Our results suggest a central role of temperature in the determination of seasonal variations in aerosol pH, consistent with the results of Tao and Murphy (Tao and Murphy, 2019) at six Canadian sites and the prediction by the multiphase buffer theory (Zheng et al., 2020). In comparison, some previous studies emphasized the importance of chemical compositions in seasonal variations (Tan et al., 2018; Ding et al., 2019), which is mainly due to the different sensitivity analysis methods applied.

带格式的: 多级符号 + 级别: 2 + 编号样式: 1, 2, 3, ... + 起始编号: 2 + 对齐方式: 左侧 + 对齐位置: 0 厘米 + 缩进位置: 0 厘米

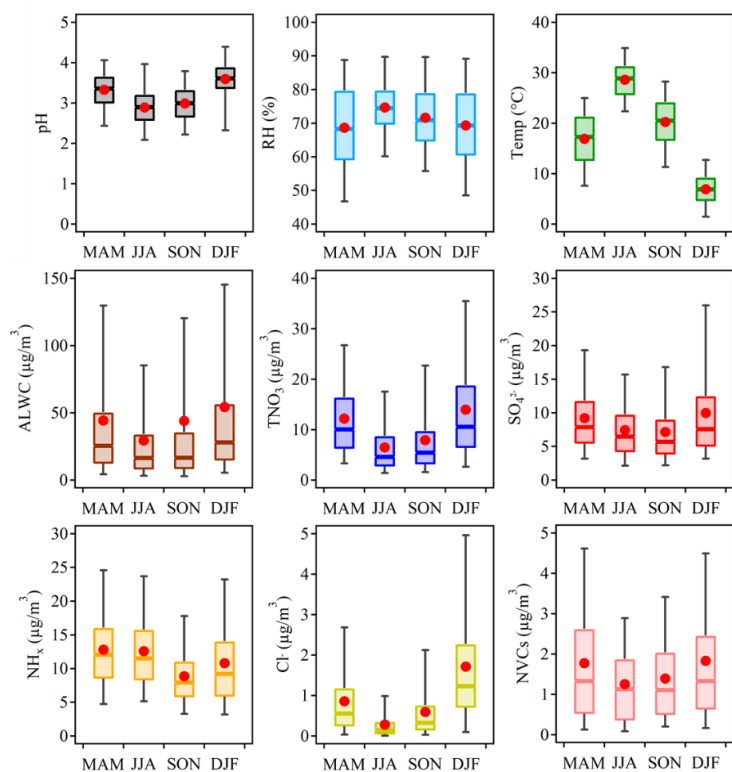


Figure 2. Seasonal patterns of the mass concentrations of major components in PM_{2.5}, relative humidity (RH), temperature (Temp), predicted aerosol liquid water content (ALWC) and aerosol pH during 2011–2019 in Shanghai.

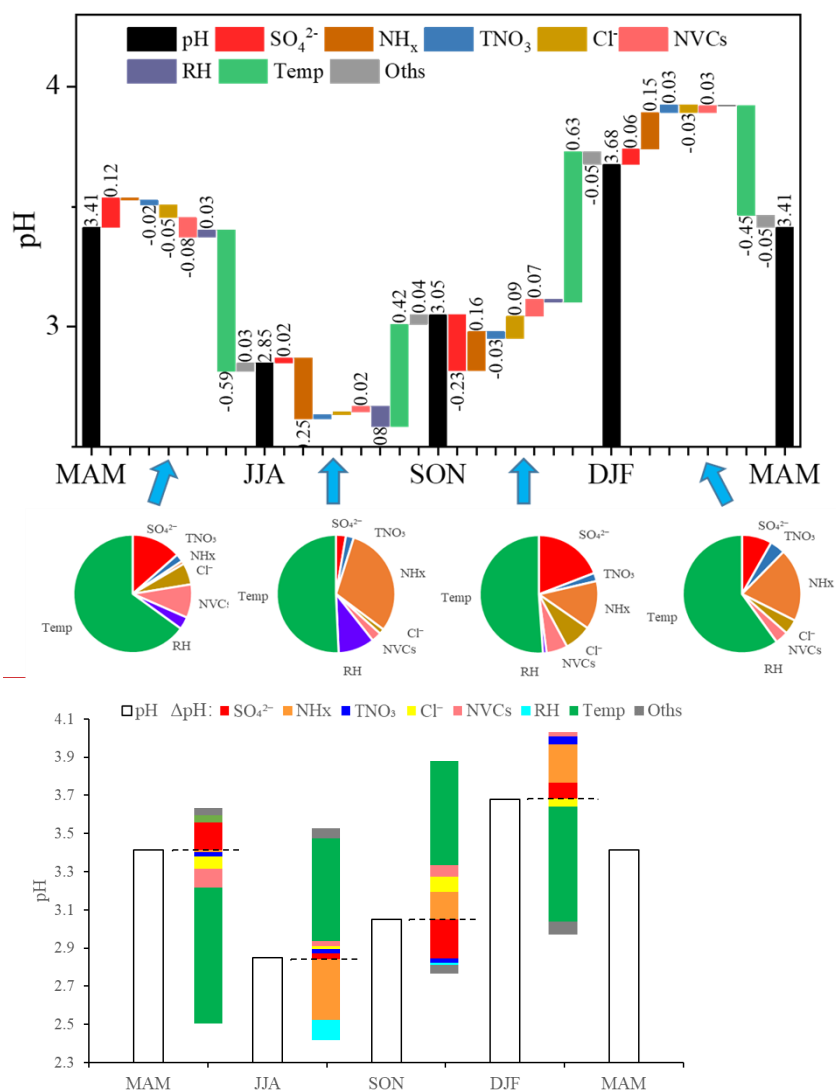


Figure 3. Contributions of individual factors to the ΔpH changes in aerosol pH across the four seasons. Here the bar plots indicate the factors contributing to the ΔpH between two adjacent seasons, e.g., spring (MAM) to summer (JJA). The meanings of the abbreviations are: RH, relative humidity; Temp, temperature; NVCs, non-volatile cations; NH_x , total ammonia; TNO_3 , total nitrate.

带格式的：居中

设置了格式：字体：小五

设置了格式：字体：非加粗

3.3 Diurnal variation

Figure 4 shows the diurnal variations in the aerosol pH and its potential drivers. ~~Similar to the results in Beijing (Tao et al., 2020), a~~ Aerosol pH in Shanghai exhibits notable diurnal variations, being higher during nighttime.

~~Figure 5 shows the effects of individual factors to the Δ pH between day and night. Here the bar plots indicate the factors contributing to the Δ pH between two adjacent hour periods, e.g., 0:00 to 6:00. See Fig. S9c for the factor contribution to the variation from average conditions. Figure 5 shows the effects of individual factors on the diurnal variations in aerosol pH. The aerosol pH was calculated from the mean averages of input parameters in 0:00, 6:00, 12:00 and 18:00, and Δ pH was estimated by varying one factor while holding the other factors fixed in different hours. Temperature and RH ~~are-were~~ among the main drivers of this diurnal variation of aerosol pH, with a max Δ pH of -0.22 and +0.10 units. As shown in Fig. 4, the maximum RH and ALWC occurred at approximately 5:00. After sunrise, increase of temperature resulted in an immediate drop of RH and ALWC with ALWC reached its lowest level in the afternoon. Accordingly, the minimum aerosol pH (~2.8) was also found in the afternoon with high temperature and low RH. After sunset, the decreasing temperature and increasing RH led to a highest aerosol pH overnight. Minor pH changes were found between 0:00 and 6:00, when temperature and RH also showed minor changes. The effects of other factors on the diurnal variations in pH were notably smaller than their effects on seasonal variations, which may be attributed to the relatively small variations of chemical profiles in the course of a day. Among these chemical factors, NH_x ~~plays-played~~ the most important roles, followed by SO_4^{2-} . Overall, temperature and RH ~~are-were~~ more important than the chemical compositions in controlling the diurnal variations in aerosol pH.~~

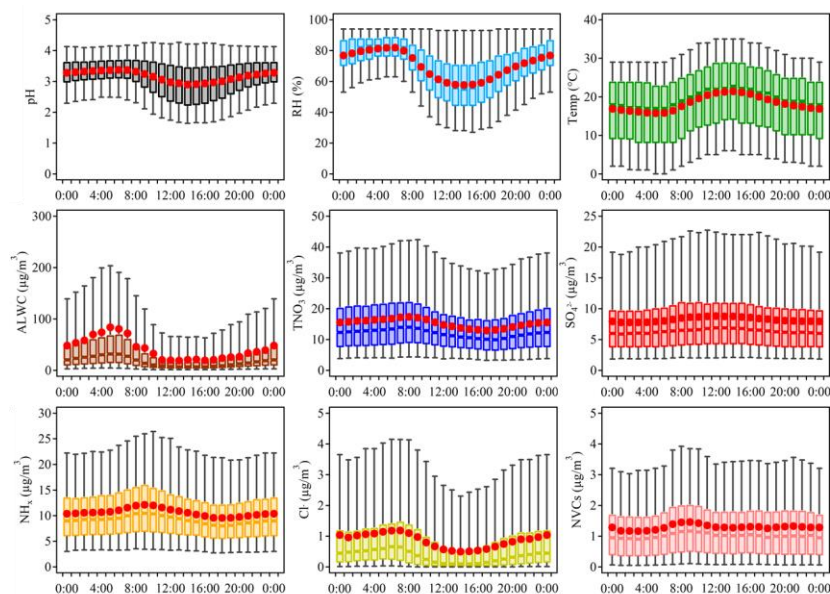


Figure 4. Diurnal patterns of the mass concentrations of major ions in PM_{2.5}, relative humidity (RH), temperature (Temp), predicted aerosol liquid water content (ALWC) and aerosol pH during 2011–2019 in Shanghai.

带格式的：缩进：首行缩进： 0 字符，行距： 1.5 倍行距

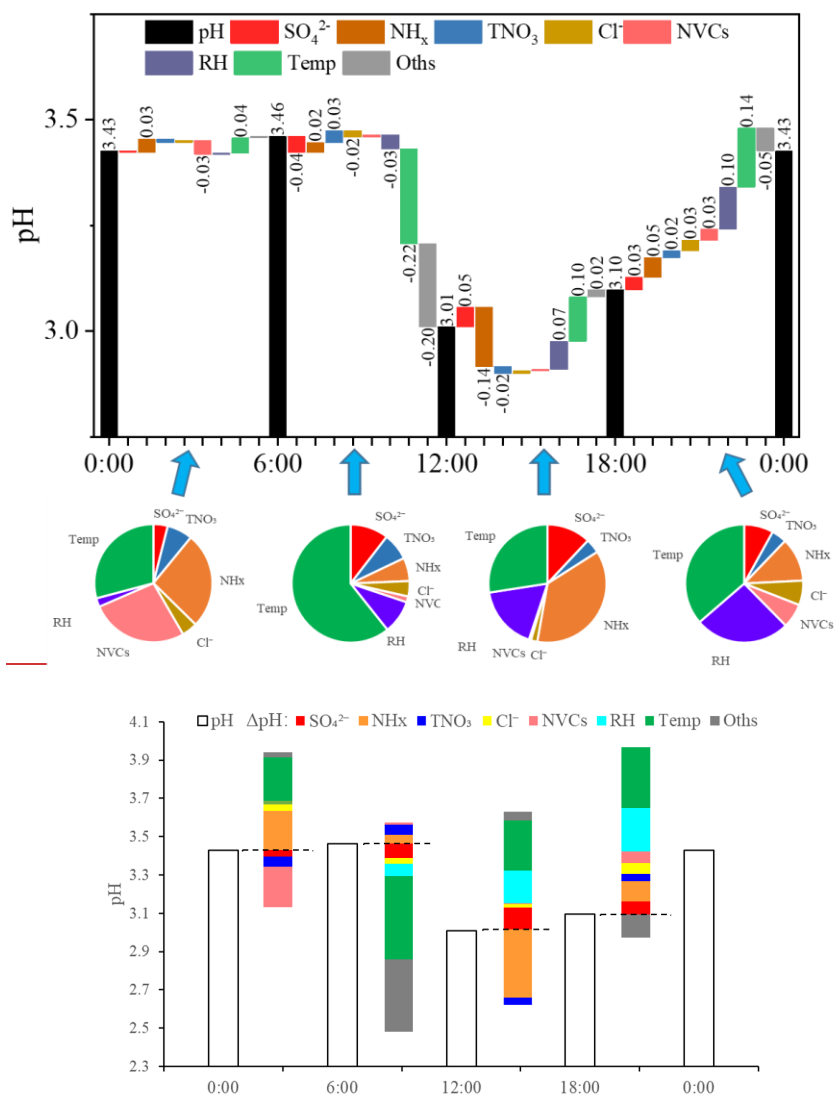


Figure 5. Fractional Contributions of individual drivers-factors to the ΔpH the aerosol pH difference between day and night. Here the bar plots indicate the factors contributing to the ΔpH between two adjacent hour periods, e.g., 0:00 to 6:00. The meanings of the abbreviations are: RH, relative humidity; Temp, temperature; NVCs, non-volatile cations; NH_x , total ammonia; TNO_3 , total nitrate.

设置了格式: 字体: 非加粗

3.4 Future projections

A series of prevention and control measures ~~are~~ have been suggested for continuous improvement of air quality, which will affect the atmospheric compositions and may subsequently affect the aerosol pH in China. To explore China's future anthropogenic emission pathways in 2015–2050, Tong et al.(2020) developed a dynamic projection model, based on which different emission scenarios were created by connecting five socio-economic pathway (SSP) scenarios, five representative concentration pathways (RCP) scenarios (RCP8.5, 7.0, 6.0, 4.5 and 2.6) and three pollution control scenarios (business as usual, BAU; enhanced control policy, ECP; and best health effect, BHE). These scenarios provide a better understanding of the future trends in pollutant emissions(Tong et al., 2020).

In this study, we chose three different emission reduction scenarios (SSP3-70-BAU, SSP2-45-ECP, and SSP1-26-BHE) as the future anthropogenic emission pathways, ~~including SSP3-70-BAU, SSP2-45-ECP and SSP1-26-BHE~~, and based on which we try~~ied~~ to project the future aerosol pH levels in Shanghai. SSP1-26-BHE, which involves a combination of strong low-carbon and air pollution control policy, has the greatest emission reduction, followed by SSP2-45-ECP. SSP3-70-BAU is a reference scenario ~~that without additional efforts to constrain emissions~~without any active actions. Figure 6 shows the emissions of SO_2 , NO_x ~~and~~, NH_3 and predicted pH levels and the changes in major chemical components (NH_4^+ , SO_4^{2-} , NO_3^- and Cl^-) in China from 2015 to 2050 under the three scenarios. We also predicted the aerosol pH based on the assumption that reductions in SO_4^{2-} , TNO_3 and NH_x are equivalent to reductions in their respective precursors (i.e., SO_2 , NO_x and NH_3).

~~As shown in Fig. 6, the future trend of aerosol pH changes little u~~Under the reference scenario weak control policy of ~~-(SSP3-70-BAU with weak control policy (blue dashed lines in Fig. 6 a-f)).~~ SO_2 and NO_x are predicted to increase, while the NH_x is relatively stable.~~Correspondingly, both SO_4^{2-} and NO_3^- will increase, and NH_4^+ will also increase in response (Fig. 6g). Considering the stable NH_x , NH_4^+ partition ratio ($\text{NH}_4^+ / (\text{NH}_4^+ + \text{NH}_3)$) will increase. In comparison, there is also little change in aerosol pH and the predicted NO_3^- partition ratio ($\text{NO}_3^- / (\text{NO}_3^- + \text{HNO}_3)$).~~

~~However, NH_4^+ partition ratio ($\text{NH}_4^+ / (\text{NH}_4^+ + \text{NH}_3)$) increases substantially, suggesting an enhanced formation of ammonium aerosols.~~ Under the moderate control policy (SSP2-45-ECP), the emissions of SO_2 , NO_x , and NH_3 in 2050 will be reduced by 62.7%, 49.0% and 25.0%, respectively.

Correspondingly, SO_4^{2-} , NO_3^- and NH_4^+ will all decrease (Fig. 6h), with a total PM reduction of $\sim 14.4 \mu\text{g m}^{-3}$. Moreover, the predicted pH will increase by ~ 0.5 , and the NO_3^- and NH_4^+ partition ratios will decrease by 0.14 and 0.23, respectively (green lines in Fig. 6d-f). That is, more nitrate and ammonium will exist in the gas phase as HNO_3 and NH_3 , thus the reduced NH_4^+ and NO_3^- is higher than the reduced NH_x and TNO_3 , which is a control bonus in terms of reduced PM per reduced emissions for this scenario.

With the strict control policy (SSP1-26-BHE), the emissions of SO_2 , NO_x and NH_3 in 2050 will decrease ~~be reduced~~ by 86.9%, 74.9% and 41.7%, respectively. Its ~~effect~~ on PM reductions resembles that of the moderate one (SSP2-45-ECP) before 2040. Afterwards, however, the NO_3^- partition ratio increased despite the increasing pH and reached near 1 in 2050 (Fig. 6 d, e). On second check, we found this pattern is due to the sharp decrease in SO_4^{2-} and constant NVCs. After 2040, there will be a major anion deficit considering the non-volatile species only (sulfate and Ca^{2+} , K^+ , Mg^{2+}), and therefore more NO_3^- will be captured by the NVCs to the particle phase. As a result, ~~and the pH will further increase to 4.30 in 2050. It is noted that the predicted pH values in the SSP1-26-BHE model decrease suddenly during 2030–2040 and then continue to rise, which is due to the decrease in ALWC and increase in pH brought by the decrease of SO_4^{2-} , TNO_3 and NH_x during 2015–2030. These variations result in a transition to the HNO_3 -sensitive regime during 2030–2040, where partitioning gradually shifts from aerosol-phase nitrate to the gaseous phase (Nenes et al., 2020a). Therefore, the decrease in TNO_3 during 2030–2040 lead to a notable decrease of pH. This can also be seen from Fig. 6e, where NO_3^- partition ratio begins to decrease gradually and reaches the HNO_3 -sensitive regime and then rises again under the strict control policy, resulting in NO_3^- partition ratio even increased from 0.92 in 2015 to 1.00 in 2050. Although According to the strict control policy, we also found that NH_4^+ partition ratio showed a continuous decrease, in 2050 both the reduced NH_4^+ and NO_3^- is smaller than the reduced NH_x and TNO_3 (Fig. 6i). That is in contrast with the effect of the moderate one (SSP2-45-ECP). Correspondingly, the total reduced PM is only slightly larger for the strict SSP1-26-BHE policy ($\sim 18.6 \mu\text{g m}^{-3}$) than the moderate SSP2-45-ECP policy ($\sim 14.4 \mu\text{g m}^{-3}$) indicating a reduced efficiency in terms of PM controls in responses to the emission controls has dropped significantly from 0.37 in 2015 to 0.02 in 2050. Because of China's commitment in reducing CO_2 , we expect a further roadmap of emission control similar to the SSP1-26-BHE scenario. In this case, the corresponding aerosol pH in eastern China will increase by ~ 0.9 , resulting in 8% more NO_3^- and 35% less NH_4^+ partitioning/formation in the aerosol phase. This would suggest a~~

reduced benefit of NH_3 and NO_x emission control in mitigating haze pollution in eastern China, especially after 2040.

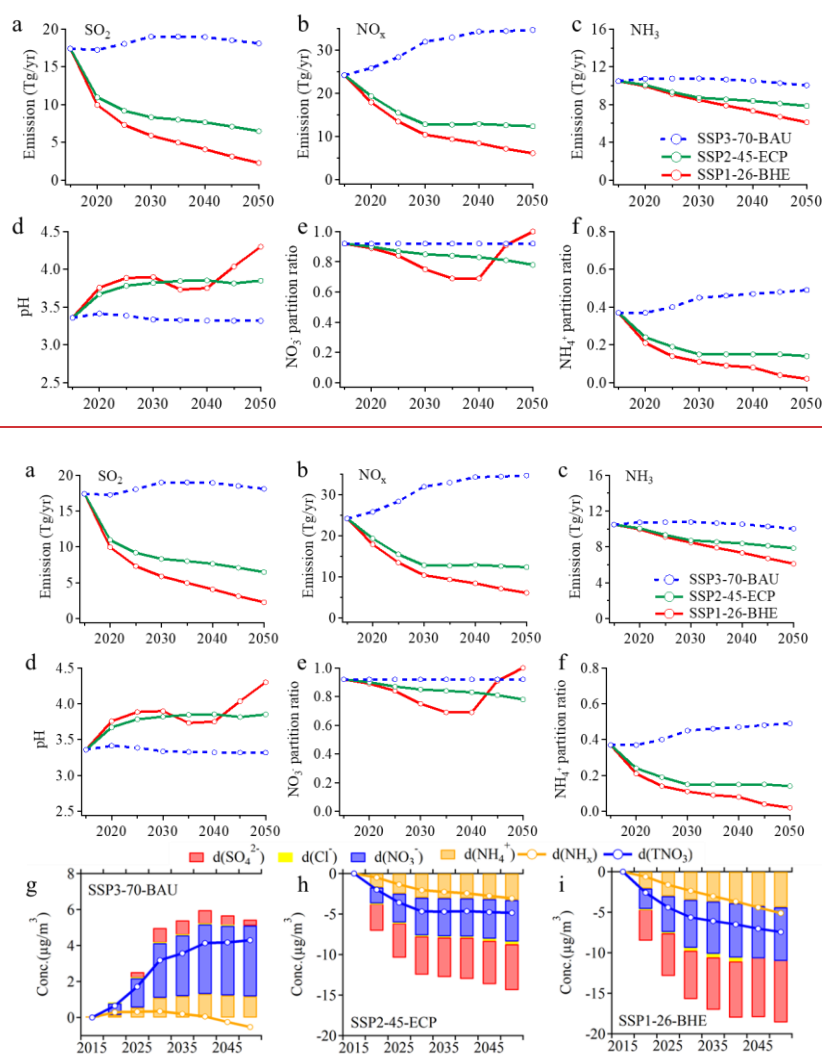


Figure 6. Emissions of SO_2 (a), NO_x (b), NH_3 (c), predicted pH (d), NO_3^- partition ($\text{NO}_3^- / (\text{NO}_3^- + \text{HNO}_3)$) (e) and NH_4^+ partition ($\text{NH}_4^+ / (\text{NH}_4^+ + \text{NH}_3)$) (f) in China from 2015 to 2050 under the three scenarios published in Tong et al. (Tong et al., 2020). Predicted the changes in major chemical components (NH_4^+ , SO_4^{2-} , NO_3^- and Cl^-) and reductions in TNO_3 and NH_x under the three scenarios, including SSP3-70-BAU (g), SSP2-45-ECP

(h) and SSP1-26-BHE (i).

4 Conclusion

The aerosol pH values at an urban site in Shanghai during 2011–2019 were calculated using ISORROPIA II. The trend analysis of aerosol pH in Shanghai during 2011–2019 was reported firstly based on observed gas and aerosol composition. Although significant variations of aerosol compositions were observed from 2011 to 2019 in YRD region, the aerosol pH estimated by model only slightly declined by 0.24 unit. The aerosol pH decreased from 3.30 ± 0.58 in 2011 to 3.06 ± 0.58 in 2019, which is related to changes in the chemical composition under the implementation of Action Plan in the YRD region. The implementation of the Action Plan leads to -35.8%, -37.6%, -9.6%, -81.0% and +1.2% changes in concentrations of $\text{PM}_{2.5}$, SO_4^{2-} , NH_x , NVCs and NO_3^- in YRD during this period. Then we quantified the contributions of individual factors to the difference in the variation of aerosol pH from 2011 to 2019. Before the implementation of the Action Plan (2011–2013), the main factors that affected the pH were the temperature and NVCs. During the implementation of the Action Plan (2013–2019), we revealed that besides the multiphase buffer effect, the opposite effects of SO_4^{2-} and non-volatile cations changes with a contribution of +0.38 and -0.35 unit on aerosol pH, respectively play a key role in determining the moderate pH trend from 2011 to 2019. SO_4^{2-} and NVCs were the most important determinants of the aerosol pH and were attributed to ΔpH of +0.38 and -0.35 units, respectively. Meanwhile, changes in NH_x and Cl^- were responsible for decreases in aerosol pH of 0.08 and 0.06 pH units, respectively, whereas the effect of TNO_3 was negligible. NH_x appeared to play an increasingly important role in determining aerosol pH through the years.

Distinct seasonal variations in the aerosol pH were observed, with maximum and minimum aerosol pH of 3.59 ± 0.57 in winter (DJF) and 2.89 ± 0.49 in summer (JJA), respectively. Seasonal variations in aerosol pH were mainly driven by the temperature, with the max ΔpH of 0.63 existed between fall and winter. Temperature through its impact on pK_a^* can largely drive the seasonal variation of aerosol pH in a multiphase-buffered system. Besides temperature, the main factors affecting the seasonal variation of aerosol pH are NH_x and SO_4^{2-} , which contributed to +16% and +12% pH change, respectively. The diurnal cycle of particle pH is driven by the combined effects of temperature and relative humidity

with a maximum which could result in ΔpH of -0.22 and +0.10 units, respectively. The effects of chemical factors on the diurnal variations in pH were notably smaller than the effects on seasonal variations, which may be attributed to the limited variations of chemical profiles in the course of a day. These results emphasized the importance of meteorological conditions in controlling the seasonal and diurnal variations of aerosol pH.

Finally, to explore the effects of China's future anthropogenic emission control pathways on aerosol pH and compositions, we chose three different emission reduction scenarios proposed by Tong et al. (2020) for future haze mitigation, naming SSP3-70-BAU, SSP2-45-ECP and SSP1-26-BHE as case studies. We estimated that the future trend of aerosol pH and NO_3^- partition ratio will change little under the weak control policy (SSP3-70-BAU), while SO_4^{2-} , NO_3^- and NH_4^+ will increase substantially. However, NH_4^+ partition ratio increases substantially, suggesting an enhanced formation of ammonium aerosols. The results also demonstrate that future aerosol pH will increase under both strict control policy (SSP1-26-BHE) and moderate control policy (SSP2-45-ECP), but more drastically under former scenario. The significant increase in aerosol pH with the strict control policy with strict control policy will lead to the reduced aerosol NH_4^+ and NO_3^- is smaller than the reduced amount of total NH_3 and total HNO_3 , which is in contrast with effect of the moderate control policy. This suggests that a reduced efficiency in terms of PM controls in responses to the emission controls with the strict control policy. These results highlight the importance of will lead to more nitrate partitioning in aerosol phase, hence inhibiting future $\text{PM}_{2.5}$ pollution control. This finding implicates that variations in aerosol pH will feedback to multiphase formation pathways of aerosols in the atmosphere. In other words, proportional reductions in precursors and follow-up variations in aerosol pH are evidently necessary to be taken into account for future efforts in mitigating haze pollution pollution control policy.

Author Contributions

HS, HW, and CH conceived and led the study. MZ conducted the field measurements and carried out the data analysis. MZ and GZ performed model simulations. MZ, HS, HW, CH, GZ, LQ, SZ, DH, YC, JA discussed the results. LQ, SZ, DH, SL, ST, QW, RY, YM, CC conducted the measurements at the station. MZ, HS and GZ wrote the manuscript with input from all co-authors.

Supplement

The supplement is available in a separate file.

Competing interests

The authors declare that they have no conflict of interest.

Data availability

The data presented in this paper are available upon request from Hang Su (h.su@mpic.de) and Cheng Huang (huangc@sacs.sh.cn).

Acknowledgement

This study was supported by the [Science and Technology Commission of Shanghai Municipality Fund Project \(20dz1204000\)](#), the National Key Research and Development Program of China (2018YFC0213800), ~~Science and Technology Commission of Shanghai Municipality Fund Project (20dz1204000)~~, the General Fund of National Natural Science Foundation of China (21806108), the National Natural Science Foundation of China (42061134008), the Shanghai Rising-Star Program (19QB1402900) and Shanghai Municipal Bureau of Ecology and Environment Fund Project (2020-03).

Reference

- Battaglia Jr, M. A., Weber, R. J., Nenes, A., and Hennigan, C. J.: Effects of water-soluble organic carbon on aerosol pH, *Atmospheric Chemistry and Physics*, 19, 14607-14620, 10.5194/acp-19-14607-2019, 2019.
- Battaglia, M. A., Douglas, S., and Hennigan, C. J.: Effect of the Urban Heat Island on Aerosol pH, *Environmental Science & Technology*, 51, 13095-13103, 10.1021/acs.est.7b02786, 2017.
- Cai, S., Wang, Y., Zhao, B., Wang, S., Chang, X., and Hao, J.: The impact of the "Air Pollution Prevention and Control Action Plan" on PM_{2.5} concentrations in Jing-Jin-Ji region during 2012-2020, *Sci Total Environ*, 580, 197-209, 10.1016/j.scitotenv.2016.11.188, 2017.
- Cheng, J., Su, J., Cui, T., Li, X., Dong, X., Sun, F., Yang, Y., Tong, D., Zheng, Y., Li, Y., Li, J., Zhang, Q., and He, K.: Dominant role of emission reduction in PM_{2.5} air quality improvement in Beijing during 2013–2017: a model-based decomposition analysis, *Atmospheric Chemistry and Physics*, 19, 6125-6146, 10.5194/acp-19-6125-2019, 2019.
- Cheng, Y., Zheng, G., Wei, C., Mu, Q., Zheng, B., Wang, Z., Gao, M., Zhang, Q., He, K., Carmichael, G., Poschl, U., and Su, H.: Reactive nitrogen chemistry in aerosol water as a source of sulfate during haze events in China, *Science Advance*, 2016.
- Clegg, S. L., Brimblecombe, P., and Wexler, A. S.: Thermodynamic Model of the System $\text{H}^+ - \text{NH}_4^+ - \text{Na}^+ - \text{SO}_4^{2-} - \text{NO}_3^- - \text{Cl}^- - \text{H}_2\text{O}$ at 298.15 K, *The Journal of Physical Chemistry A*, 102, 2155-2171, 10.1021/jp973043j, 1998.

Ding, J., Zhao, P., Su, J., Dong, Q., Du, X., and Zhang, Y.: Aerosol pH and its driving factors in Beijing, *Atmospheric Chemistry and Physics*, 19, 7939-7954, 10.5194/acp-19-7939-2019, 2019.
 Fang, T., Guo, H., Zeng, L., Verma, V., Nenes, A., and Weber, R. J.: Highly Acidic Ambient Particles, Soluble Metals, and Oxidative Potential: A Link between Sulfate and Aerosol Toxicity, *Environ Sci Technol*, 51, 2611-2620, 10.1021/acs.est.6b06151, 2017.
 Fountoukis, C. and Nenes, A.: ISORROPIA II: a computationally efficient thermodynamic equilibrium model for $K^+Ca^{2+}Mg^{2+}NH_4^+Na^+SO_4^{2-}NO_3^-Cl^-H_2O$ aerosols, *Atmospheric Chemistry and Physics*, 7, 4639-4659, 2007.
 Fu, X., Guo, H., Wang, X., Ding, X., He, Q., Liu, T., and Zhang, Z.: PM_{2.5} acidity at a background site in the Pearl River Delta region in fall-winter of 2007-2012, *J Hazard Mater*, 286, 484-492, 10.1016/j.jhazmat.2015.01.022, 2015.
 Guo, H., Weber, R. J., and Nenes, A.: High levels of ammonia do not raise fine particle pH sufficiently to yield nitrogen oxide-dominated sulfate production, *Sci Rep*, 7, 12109, 10.1038/s41598-017-11704-0, 2017a.
 Guo, H., Otjes, R., Schlag, P., Kiendler-Scharr, A., Nenes, A., and Weber, R. J.: Effectiveness of ammonia reduction on control of fine particle nitrate, *Atmospheric Chemistry and Physics*, 18, 12241-12256, 10.5194/acp-18-12241-2018, 2018.
 Guo, H., Liu, J., Froyd, K. D., Roberts, J. M., Veres, P. R., Hayes, P. L., Jimenez, J. L., Nenes, A., and Weber, R. J.: Fine particle pH and gas-particle phase partitioning of inorganic species in Pasadena, California, during the 2010 CalNex campaign, *Atmospheric Chemistry and Physics*, 17, 5703-5719, 10.5194/acp-17-5703-2017, 2017b.
 Guo, H., Sullivan, A. P., Campuzano-Jost, P., Schroder, J. C., Lopez-Hilfiker, F. D., Dibb, J. E., Jimenez, J. L., Thornton, J. A., Brown, S. S., Nenes, A., and Weber, R. J.: Fine particle pH and the partitioning of nitric acid during winter in the northeastern United States, *Journal of Geophysical Research: Atmospheres*, 121, 3355-3376, 10.1002/2016jd025311, 2016.
 Guo, H., Xu, L., Bougiatioti, A., Cerully, K. M., Capps, S. L., Hite, J. R., Carlton, A. G., Lee, S. H., Bergin, M. H., Ng, N. L., Nenes, A., and Weber, R. J.: Fine-particle water and pH in the southeastern United States, *Atmospheric Chemistry and Physics*, 15, 5211-5228, 10.5194/acp-15-5211-2015, 2015.
 He, P., Alexander, B., Geng, L., Chi, X., Fan, S., Zhan, H., Kang, H., Zheng, G., Cheng, Y., Su, H., Liu, C., and Xie, Z.: Isotopic constraints on heterogeneous sulfate production in Beijing haze, *Atmospheric Chemistry and Physics*, 18, 5515-5528, 10.5194/acp-18-5515-2018, 2018.
 Hennigan, C. J., Izumi, J., Sullivan, A. P., Weber, R. J., and Nenes, A.: A critical evaluation of proxy methods used to estimate the acidity of atmospheric particles, *Atmospheric Chemistry and Physics*, 15, 2775-2790, 10.5194/acp-15-2775-2015, 2015.
 Huang, X. H. H., Bian, Q., Ng, W. M., Louie, P. K. K., and Yu, J. Z.: Characterization of PM_{2.5} Major Components and Source Investigation in Suburban Hong Kong: A One Year Monitoring Study, *Aerosol and Air Quality Research*, 14, 237-250, 10.4209/aaqr.2013.01.0020, 2014.
 Jia, S., Wang, X., Zhang, Q., Sarkar, S., Wu, L., Huang, M., Zhang, J., and Yang, L.: Technical note: Comparison and interconversion of pH based on different standard states for aerosol acidity characterization, *Atmospheric Chemistry and Physics*, 18, 11125-11133, 10.5194/acp-18-11125-2018, 2018.
 Li, C., Hu, Y., Chen, J., Ma, Z., Ye, X., Yang, X., Wang, L., Wang, X., and Mellouki, A.: Physicochemical properties of carbonaceous aerosol from agricultural residue burning: Density,

volatility, and hygroscopicity, *Atmospheric Environment*, 140, 94-105, 10.1016/j.atmosenv.2016.05.052, 2016.

Li, H., Cheng, J., Zhang, Q., Zheng, B., Zhang, Y., Zheng, G., and He, K.: Rapid transition in winter aerosol composition in Beijing from 2014 to 2017: response to clean air actions, *Atmospheric Chemistry and Physics*, 19, 11485-11499, 10.5194/acp-19-11485-2019, 2019.

Li, W., Xu, L., Liu, X., Zhang, J., Lin, Y., Yao, X., Gao, H., Zhang, D., Chen, J., Wang, W., Harrison, R. M., Zhang, X., Shao, L., Fu, P., Nenes, A., and Shi, Z.: Air pollution–aerosol interactions produce more bioavailable iron for ocean ecosystems, *Science Advance*, 3, e1601749, 2017.

Liu, M., Huang, X., Song, Y., Xu, T., Wang, S., Wu, Z., Hu, M., Zhang, L., Zhang, Q., Pan, Y., Liu, X., and Zhu, T.: Rapid SO₂ emission reductions significantly increase tropospheric ammonia concentrations over the North China Plain, *Atmospheric Chemistry and Physics*, 18, 17933-17943, 10.5194/acp-18-17933-2018, 2018.

Masiol, M., Squizzato, S., Formenton, G., Khan, M. B., Hopke, P. K., Nenes, A., Pandis, S. N., Tositti, L., Benetello, F., Visin, F., and Pavoni, B.: Hybrid multiple-site mass closure and source apportionment of PM_{2.5} and aerosol acidity at major cities in the Po Valley, *Sci Total Environ*, 704, 135287, 10.1016/j.scitotenv.2019.135287, 2020.

Nah, T., Guo, H., Sullivan, A. P., Chen, Y., Tanner, D. J., Nenes, A., Russell, A., Ng, N. L., Huey, L. G., and Weber, R. J.: Characterization of aerosol composition, aerosol acidity, and organic acid partitioning at an agriculturally intensive rural southeastern US site, *Atmospheric Chemistry and Physics*, 18, 11471-11491, 10.5194/acp-18-11471-2018, 2018.

Nenes, A., Pandis, S. N., Weber, R. J., and Russell, A.: Aerosol pH and liquid water content determine when particulate matter is sensitive to ammonia and nitrate availability, *Atmospheric Chemistry and Physics*, 20, 3249-3258, 10.5194/acp-20-3249-2020, 2020a.

Nenes, A., Pandis, S. N., Kanakidou, M., Russell, A., Song, S., Vasilakos, P., and Weber, R. J.: Aerosol acidity and liquid water content regulate the dry deposition of inorganic reactive nitrogen, *Atmospheric Chemistry and Physics Discussion*, 10.5194/acp-2020-266, 2020b.

Pye, H. O. T., Zuend, A., Fry, J. L., Isaacman-VanWertz, G., Capps, S. L., Appel, K. W., Foroutan, H., Xu, L., Ng, N. L., and Goldstein, A. H.: Coupling of organic and inorganic aerosol systems and the effect on gas-particle partitioning in the southeastern US, *Atmos Chem Phys*, 18, 357-370, 10.5194/acp-18-357-2018, 2018.

Pye, H. O. T., Nenes, A., Alexander, B., Ault, A. P., Barth, M. C., Clegg, S. L., Collett Jr, J. L., Fahey, K. M., Hennigan, C. J., Herrmann, H., Kanakidou, M., Kelly, J. T., Ku, I. T., McNeill, V. F., Riemer, N., Schaefer, T., Shi, G., Tilgner, A., Walker, J. T., Wang, T., Weber, R., Xing, J., Zaveri, R. A., and Zuend, A.: The acidity of atmospheric particles and clouds, *Atmospheric Chemistry and Physics*, 20, 4809-4888, 10.5194/acp-20-4809-2020, 2020.

Qiao, L., Cai, J., Wang, H., Wang, W., Zhou, M., Lou, S., Chen, R., Dai, H., Chen, C., and Kan, H.: PM_{2.5} constituents and hospital emergency-room visits in Shanghai, China, *Environ Sci Technol*, 48, 10406-10414, 10.1021/es501305k, 2014.

Rumsey, I. C., Cowen, K. A., Walker, J. T., Kelly, T. J., Hanft, E. A., Mishoe, K., Rogers, C., Proost, R., Beachley, G. M., Lear, G., Frelink, T., and Otjes, R. P.: An assessment of the performance of the Monitor for AeRosols and Gases in ambient air (MARGA): a semi-continuous method for soluble compounds, *Atmospheric Chemistry and Physics*, 14, 5639-5658, 10.5194/acp-14-5639-2014, 2014.

Shi, X., Nenes, A., Xiao, Z., Song, S., Yu, H., Shi, G., Zhao, Q., Chen, K., Feng, Y., and Russell, A. G.: High-Resolution Data Sets Unravel the Effects of Sources and Meteorological Conditions on

Nitrate and Its Gas-Particle Partitioning, *Environ Sci Technol*, 53, 3048-3057, 10.1021/acs.est.8b06524, 2019.

Song, S., Gao, M., Xu, W., Shao, J., Shi, G., Wang, S., Wang, Y., Sun, Y., and McElroy, M. B.: Fine-particle pH for Beijing winter haze as inferred from different thermodynamic equilibrium models, *Atmospheric Chemistry and Physics*, 18, 7423-7438, 10.5194/acp-18-7423-2018, 2018.

Stieger, B., Spindler, G., Fahlbusch, B., Müller, K., Grüner, A., Poulain, L., Thöni, L., Seidler, E., Wallasch, M., and Herrmann, H.: Measurements of PM10 ions and trace gases with the online system MARGA at the research station Melpitz in Germany – A five-year study, *Journal of Atmospheric Chemistry*, 75, 33-70, 10.1007/s10874-017-9361-0, 2018.

Su, H., Cheng, Y., and Poschl, U.: New Multiphase Chemical Processes Influencing Atmospheric Aerosols, Air Quality, and Climate in the Anthropocene, *Acc Chem Res*, 53, 2034-2043, 10.1021/acs.accounts.0c00246, 2020.

Tan, T., Hu, M., Li, M., Guo, Q., Wu, Y., Fang, X., Gu, F., Wang, Y., and Wu, Z.: New insight into PM2.5 pollution patterns in Beijing based on one-year measurement of chemical compositions, *Sci Total Environ*, 621, 734-743, 10.1016/j.scitotenv.2017.11.208, 2018.

Tao, W., Su, H., Zheng, G., Wang, J., Wei, C., Liu, L., Ma, N., Li, M., Zhang, Q., Pöschl, U., and Cheng, Y.: Aerosol pH and chemical regimes of sulfate formation in aerosol water during winter haze in the North China Plain, *Atmospheric Chemistry and Physics*, 20, 11729-11746, 10.5194/acp-20-11729-2020, 2020.

Tao, Y. and Murphy, J. G.: The sensitivity of PM2.5 acidity to meteorological parameters and chemical composition changes: 10-year records from six Canadian monitoring sites, *Atmos. Chem. Phys.*, 19, 9309-9320, 10.5194/acp-19-9309-2019, 2019.

Tilgner, A., Schaefer, T., Alexander, B., Barth, M., Collett Jr, J. L., Fahey, K. M., Nenes, A., Pye, H. O. T., Herrmann, H., and McNeill, V. F.: Acidity and the multiphase chemistry of atmospheric aqueous particles and clouds, *Atmospheric Chemistry and Physics*, 21, 13483-13536, 10.5194/acp-21-13483-2021, 2021.

Tong, D., Cheng, J., Liu, Y., Yu, S., Yan, L., Hong, C., Qin, Y., Zhao, H., Zheng, Y., Geng, G., Li, M., Liu, F., Zhang, Y., Zheng, B., Leon, C., and Zhang, Q.: Dynamic projection of anthropogenic emissions in China: methodology and 2015–2050 emission pathways under a range of socio-economic, climate policy, and pollution control scenarios, *Atmospheric Chemistry and Physics*, 20, 5729-5757, 10.5194/acp-20-5729-2020, 2020.

Vasilakos, P., Russell, A., Weber, R., and Nenes, A.: Understanding nitrate formation in a world with less sulfate, *Atmospheric Chemistry and Physics*, 18, 12765-12775, 10.5194/acp-18-12765-2018, 2018.

Wang, H., Ding, J., Xu, J., Wen, J., Han, J., Wang, K., Shi, G., Feng, Y., Ivey, C. E., Wang, Y., Nenes, A., Zhao, Q., and Russell, A. G.: Aerosols in an arid environment: The role of aerosol water content, particulate acidity, precursors, and relative humidity on secondary inorganic aerosols, *Sci Total Environ*, 646, 564-572, 10.1016/j.scitotenv.2018.07.321, 2019.

Wang, S., Wang, L., Li, Y., Wang, C., Wang, W., Yin, S., and Zhang, R.: Effect of ammonia on fine-particle pH in agricultural regions of China: comparison between urban and rural sites, *Atmospheric Chemistry and Physics*, 20, 2719-2734, 10.5194/acp-20-2719-2020, 2020.

Weber, R. J., Guo, H., Russell, A. G., and Nenes, A.: High aerosol acidity despite declining atmospheric sulfate concentrations over the past 15 years, *Nature Geoscience*, 9, 282-285, 10.1038/ngeo2665, 2016.

586 Xie, Y., Wang, G., Wang, X., Chen, J., Chen, Y., Tang, G., Wang, L., Ge, S., Xue, G., Wang, Y., and
 587 Gao, J.: Nitrate-dominated PM_{2.5} and elevation of particle pH observed in urban Beijing during the
 588 winter of 2017, *Atmospheric Chemistry and Physics*, 20, 5019-5033, 10.5194/acp-20-5019-2020,
 589 2020.
 590 Zheng, B., Tong, D., Li, M., Liu, F., Hong, C., Geng, G., Li, H., Li, X., Peng, L., Qi, J., Yan, L.,
 591 Zhang, Y., Zhao, H., Zheng, Y., He, K., and Zhang, Q.: Trends in China's anthropogenic emissions
 592 since 2010 as the consequence of clean air actions, *Atmospheric Chemistry and Physics*, 18, 14095-
 593 14111, 10.5194/acp-18-14095-2018, 2018.
 594 Zheng, G., Su, H., Wang, S., Andreae, M. O., Poschl, U., and Cheng, Y.: Multiphase buffer theory
 595 explains contrasts in atmospheric aerosol acidity, *Science* 369, 1374-1377, 2020.
 596 Zhou, M., Qiao, L., Zhu, S., Li, L., Lou, S., Wang, H., Wang, Q., Tao, S., Huang, C., and Chen, C.:
 597 Chemical characteristics of fine particles and their impact on visibility impairment in Shanghai
 598 based on a 1-year period observation, *J Environ Sci (China)*, 48, 151-160, 10.1016/j.jes.2016.01.022,
 599 2016.
 600